

RESEARCH

Open Access



A promising natural killer cell-based model and a nomogram for the prognostic prediction of clear-cell renal cell carcinoma

Qinfan Yao^{1,2,3,4}, Xiuyuan Zhang^{1,2,3,4}, Yucheng Wang^{1,2,3,4}, Cuili Wang^{1,2,3,4}, Jianghua Chen^{1,2,3,4*} and Dajin Chen^{1,2,3,4*}

Abstract

Background Clear-cell renal cell carcinoma (ccRCC) is one of prevalent kidney malignancies with an unfavorable prognosis. There is a need for a robust model to predict ccRCC patient survival and guide treatment decisions.

Methods RNA-seq data and clinical information of ccRCC were obtained from the TCGA and ICGC databases. Expression profiles of genes related to natural killer (NK) cells were collected from the Immunology Database and Analysis Portal database. Key NK cell-related genes were identified using consensus clustering algorithms to classify patients into distinct clusters. A NK cell-related risk model was then developed using Least Absolute Shrinkage and Selection Operator (LASSO) Cox regression to predict ccRCC patient prognosis. The relationship between the NK cell-related risk score and overall survival, clinical features, tumor immune characteristics, as well as response to commonly used immunotherapies and chemotherapy, was explored. Finally, the NK cell-related risk score was validated using decision tree and nomogram analyses.

Results ccRCC patients were stratified into 3 molecular clusters based on expression of NK cell-related genes. Significant differences were observed among the clusters in terms of prognosis, clinical characteristics, immune infiltration, and therapeutic response. Furthermore, six NK cell-related genes (DPYSL3, SLPI, SLC44A4, ZNF521, LIMCH1, and AHR) were identified to construct a prognostic model for ccRCC prediction. The high-risk group exhibited poor survival outcomes, lower immune cell infiltration, and decreased sensitivity to conventional chemotherapies and immunotherapies. Importantly, the quantitative real-time polymerase chain reaction (qRT-PCR) confirmed significantly high DPYSL3 expression and low SLC44A4 expression in ACHN cells. Finally, the decision tree and nomogram consistently show the dramatic prediction performance of the risk score on the survival outcome of the ccRCC patients.

Conclusions The six-gene model based on NK cell-related gene expression was validated and found to accurately mirror immune microenvironment and predict clinical outcomes, contributing to enhanced risk stratification and therapy response for ccRCC patients.

Keywords Clear-cell renal cell carcinoma, Natural killer cells, TCGA, Risk score, Prognosis

*Correspondence:

Jianghua Chen
chenjianghua@zju.edu.cn
Dajin Chen
zju2001@zju.edu.cn

Full list of author information is available at the end of the article



© The Author(s) 2024. **Open Access** This article is licensed under a Creative Commons Attribution 4.0 International License, which permits use, sharing, adaptation, distribution and reproduction in any medium or format, as long as you give appropriate credit to the original author(s) and the source, provide a link to the Creative Commons licence, and indicate if changes were made. The images or other third party material in this article are included in the article's Creative Commons licence, unless indicated otherwise in a credit line to the material. If material is not included in the article's Creative Commons licence and your intended use is not permitted by statutory regulation or exceeds the permitted use, you will need to obtain permission directly from the copyright holder. To view a copy of this licence, visit <http://creativecommons.org/licenses/by/4.0/>. The Creative Commons Public Domain Dedication waiver (<http://creativecommons.org/publicdomain/zero/1.0/>) applies to the data made available in this article, unless otherwise stated in a credit line to the data.

Introduction

Clear-cell renal cell carcinoma (ccRCC) represents the most prevalent histological subtype of renal cell carcinoma (RCC), accounting for over 70% of the cases worldwide [1–5]. With its high invasiveness and recurrence, ccRCC annually causes more than 175,000 mortality rates worldwide and a poor 5-year survival probability of approximately 50% [6–10]. Although partial or radical nephrectomy is currently the optimal choice for ccRCC, about 25% of patients present with lymph node or distant metastasis at the first diagnosis and are unable to undergo surgery, while over 30% of ccRCC patients experience relapse and metastases after surgery [11–13]. The considerable exploration of prognostic models of ccRCC and the wide application of immune checkpoint-blocking therapies have gradually shown powerful potential and may offer new therapeutic options for ccRCC patients [14–18]. Emerging evidence has proven that immune cells serve an essential function in ccRCC pathogenesis, providing a novel outlook into immunotherapy for ccRCC [19–22]. The previously constructed immune/stromal scores have indicated a strong association between ccRCC prognosis monitoring and precision immunotherapy [23]. And the 3 immune infiltration patterns of ccRCC showed that ccRCC had the highest immune infiltration and T cell infiltration score [24]. Importantly, the complete single-cell chromatin chart of immune cells in ccRCC assisted us in better understanding immune cell functional states in ccRCC [25]. Meanwhile, several single-cell sequencing analyses provided an in-depth knowledge of the immune landscape and immune cell infiltration patterns of ccRCC, which contributed to setting a foundation for the theoretical basis of targeted therapy [26–28].

Recently, natural killer (NK) cells have been shown to play a critical role in immune surveillance against viruses, bacterial infections, and tumors [29–31]. NK cells encode both activating and inhibitory receptors and further integrate diverse signaling pathways to exert corresponding functional outcomes, especially in the production of cytokines and chemokines [32–34]. The significant advances in NK-cell biology and the gradual unveiling of molecular mechanisms have provided novel strategies involving the regulation of NK activation and cancer cell recognition, which are considered as important for cancer immunotherapy [35–39]. Moreover, immune cell-based prognostic models have been widely explored in clinical settings for guiding cancer management [40–42]. An increasing number of NK cell-related genes are being widely studied for their important roles in various types of tumors. For example, NKG2D, NKp30, and NKp46 trigger cytotoxic effects by binding to ligands on the surface of tumor cells, thus exerting anti-tumor effects

[43–45]. And NK cells are recognized as a significant prognostic factor for multiple cancers. In gastric cancer, researchers have found that abnormal percentage of NK cell in peripheral blood predicts patients' poor survival rates [46]. In triple-negative breast cancer, a 5-NK cell-related gene model also exhibit powerful value for prognosis prediction and immunotherapy evaluation [47]. However, there is currently no comprehensive understanding on the role of NK cell-related genes in ccRCC.

Therefore, the objective of this study is to investigate the role of NK cells in the carcinogenesis process of ccRCC, and to evaluate the potential value of targeting NK cell-related genes for optimizing risk stratification and predicting treatment efficacy in ccRCC. We estimated associations between the expression features and functional features of NK cell-related genes with ccRCC, and constructed a prognostic risk model to estimate the tumor immune microenvironment, predict prognosis, explore the treatment response, and allow for risk stratification. Our findings can aid in accurate therapeutic decisions being made for ccRCC patients.

Materials and methods

Data collection and processing

The transcriptome RNA-sequencing (RNA-seq) data and relevant clinical information on ccRCC were retrieved from TCGA-KIRC project of the Cancer Genome Atlas (TCGA) database (<https://portal.gdc.cancer.gov/projects/TCGA-KIRC>). Total 134 genes associated with natural killer cells were obtained from the Immunology Database and Analysis Portal (ImmPort) database (<https://www.immport.org/home>) [48]. The RECA-EU database of the International Cancer Genome Consortium (ICGC) database was searched to obtain the corresponding RNA-seq data and clinical information (<https://dcc.icgc.org/projects/RECA-EU>) as validation set.

Cell culture and qRT-PCR analysis

Human ccRCC ACHN cells and kidney proximal tubular epithelial (HK2) cells were cultivated in Dulbecco's modified Eagle's medium (DMEM) with 10% fetal bovine serum (FBS) and 1% penicillin–streptomycin. All cells were cultured under humidified conditions at 5% CO₂ and at 37 °C. We conducted a qRT-PCR to quantify the expression of the genes selected to be used in the model. Total RNA was obtained from the cultured cells using TRIzol reagent (Invitrogen, CA, USA). The PrimeScriptTM RT reagent kit (Takara, Shiga, Japan) was applied to reverse transcribe the RNA into complementary DNA (cDNA), following the manufacturer's instructions [49]. Sequences of all primers used are presented in Additional file 1: Table S1. The experiments on each gene were performed in triplicate and the average cycle threshold (Ct)

was computed. The mRNA levels were normalized to that of the housekeeping gene, GAPDH, using the $2^{-\Delta\Delta Ct}$ method.

Identification of NK cell-related genes specific to ccRCC prognosis and the establishment of a molecular cluster

A univariate Cox regression model analysis was performed on the TCGA database to select prognostic genes among the NK cell-related genes using the R package survival “coxph” function. Then, the R package, ‘Consensus-ClusterPlus’, was used to construct a consistency matrix and classify the ccRCC samples in TCGA dataset into distinct molecular clusters. The optimal number of clustering was identified using the cumulative distribution function (CDF) curve [50]. Kaplan–Meier survival analysis was performed to estimate the prognosis of patients in each molecular cluster.

Relationships between molecular clusters and clinical features, immune infiltration, and treatment response

Moreover, we also explored the distribution of clinical-pathological features among the distinct molecular clusters using a Chi-square test and one-way analysis of variance (ANOVA) using SPSS version 20.0 (SPSS Inc., Chicago, IL). To describe the differences of immune cell infiltration and the abundance of stromal cells in each distinct cluster, we implemented the R package, microenvironment cell populations-counter (MCP-counter) [51], single-sample gene set enrichment analysis (ssGSEA) [52], as well as the Estimation of Stromal and Immune cells in Malignant Tumors using Expression data (ESTIMATE) algorithm [53]. Meanwhile, we assessed the immunotherapeutic response of each cluster to immune checkpoint blockade (ICB) using the Tumor Immune Dysfunction and Exclusion (TIDE) algorithm [54]. In addition, IC50 concentrations were also assessed using the R package, ‘pRRophetic’, to measure the sensitivity of the ccRCC patients in each cluster to several chemotherapeutic agents in the GDSC database (Genomics of Drug Sensitivity in Cancer, <https://www.cancerrxgene.org/>).

Establishment of a NK cell-related model

Based on the above molecular clusters, we performed differential gene expression (DGE) analysis on each couple of clusters using the R package, ‘limma’. The selection criteria were log fold change (FC) > 1 and adjusted p -value < 0.05. Then, we took the intersection between the significantly differential expressed NK cell-related genes (DE-NKRGs) of each cluster. The univariate Cox analysis was used to identify the DE-NKRGs with a threshold of $p < 0.001$. To construct the prognostic model, least absolute shrinkage and selection operator (LASSO) regression were performed on the TCGA database using

the R package, ‘glmnet’. Based on the minimum criteria, the optimal tuning parameter λ and coefficients were calculated through tenfold cross-validation. The multivariable stepwise Cox regression model was further used to identify parameter values using the Akaike information criterion (AIC). Then, a prognostic gene model was constructed based on the linear combination of the LASSO regression coefficient (β) weighted by its mRNA expression level. The patients were divided into high-risk or low-risk groups based on the median score. Meanwhile, the ROC curve was constructed using the R package, ‘time ROC’ to estimate model performance. The Kaplan–Meier (KM) curve was analyzed using the R package, ‘survival’ to analyze the outcomes of both groups. Finally, we used the ICGC database to validate the prognostic value and robustness of the model.

Relationships between risk score and clinical characteristics, immune infiltration, and therapeutic effects

The relationships between the risk score and multiple clinical factors, including neoadjuvant status, sex, and age, were estimated. Subsequently, we employed the MCP-counter method to compare the degree of immune cell infiltration between the high- and low-risk groups of the TCGA cohort. It is generally known that differences in the expression of immune checkpoint genes influence the response after immune checkpoint inhibitor treatment in malignant tumors. Therefore, we evaluated differences in the expression levels of the immune checkpoints downloaded from the HisgAtlas database (<http://biokb.ncpsb.org/HisgAtlas/>) between two risky groups [55]. The TIDE algorithm was further used to analyze the efficacy of immunotherapy. To explore the sensitivity to different types of treatments in each risk group of TCGA cohort, ridge regression was applied to assess the IC50 of the chemotherapy drugs.

Predictive decision-tree model and nomogram construction

To explore the importance of the risk score and clinical factors, 4 clinical factors, age, gender, grade, and TNM stage, were extracted from the above analysis and used as input features, and were used along with the risk score to construct the decision tree model using R package, ‘rpart’. Univariate and multivariate Cox regression analyses were further performed to identify significant prognostic factors for ccRCC. Furthermore, the nomogram model, which integrated clinical features (age, gender, and tumor stage) and the risk score, was constructed using the R package, ‘rms’, to clearly and precisely predict the 1-, 3-, and 5-year outcomes of the patients [56]. Subsequently, the calibration curves were used to test the performance of the nomogram against the actual survival rate. Finally,

time-dependent (tROC) analysis was performed using the R package, 'survivalROC' to estimate the predictive power of the nomogram, stage, grade, TNM stage, age, and risk score [57].

Statistical analysis

Statistical analyses were performed using R version 4.0.4 and SPSS 26.0 software, while figures were drawn using GraphPad Prism 8.4.2 software. Differences between groups were compared using the Wilcoxon test or Kruskal–Wallis test. A *p* value < 0.05 was considered to indicate statistical significance in all analyses.

Results

Molecular clusters of ccRCC based on the NK cell-related genes

First, univariate Cox regression analysis was used to screen the NK cell-related genes that were significantly associated with the prognosis of ccRCC data obtained from the TCGA database. Overall, 55 genes were selected based on their prognostic value, including 18 hazardous genes and 37 protective genes (Fig. 1a). Based on the expression levels of these 55 genes, we conducted a

consensus clustering analysis on the ccRCC patients to better understand the role of the NK cell-related genes in ccRCC. We continuously increased the clustering variable *k* from 2 to 9, and found that *k*=3 produced the ideal cumulative distribution function (CDF) value and delta area (Fig. 1b, c). Therefore, the patients in the TCGA cohort were divided into 3 clusters of NK-related genes: C1, C2, and C3 (Fig. 1d). KM analysis illustrated that C2 genes increased overall survival (OS) and that the C3 patients had relatively poorer outcomes (Fig. 1e).

Comparison of clinical features, immune characteristics of TME, and the therapeutic response between the 3 molecular clusters

The distribution of clinical features among the 3 clusters showed that differences exist based on the stage, grade, T stage, M stage, age, and gender of the 3 clusters in the TCGA database. Patients younger than 60 years with less advanced tumor stages were more concentrated in the C2 cluster (Additional file 1: Fig. S1A). Additionally, the interaction between the tumor immune microenvironment and cancer cells determined cancer progression and the efficacy of immunotherapy. The MCP-Counter

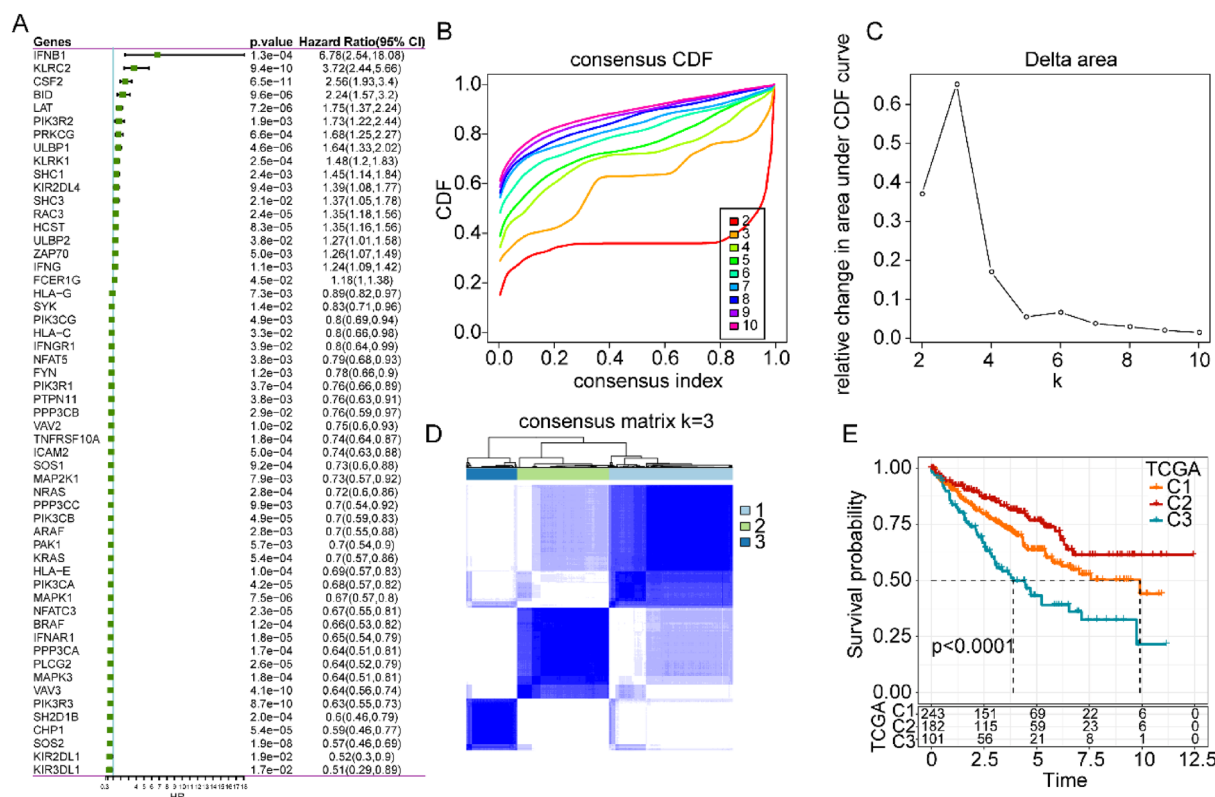


Fig. 1 Development of molecular clusters based on the expression of NK cell-related gene in ccRCC using the TCGA database. **A** Univariate Cox analysis of 134 NK cell-related genes. **B** CDF curves for *k* ranging from 2 to 9. **C** Corresponding change in the area under the CDF curve. **D** Consensus clustering matrix for the optimal, *k*=3. **E** Kaplan–Meier survival analysis of patients in cluster 1, cluster 2, and cluster 3

algorithm was applied to identify the degree of infiltration of 10 immune cells and it was found that the immune scores were highest in the C2 cluster (Additional file 1: Fig. S1B). Through the ESTIMATE method, we also found significant differences in the infiltration of stromal and immune cells into tumor tissues. The results revealed that the C2 cluster possessed higher stromal and immune scores (Additional file 1: Fig. S1C). Based on these immune features, we determined the expression of immune checkpoint genes and most immune checkpoint genes were found to be highly expressed in the C2 cluster (Additional file 1: Fig. S1D). To further evaluate patient populations that may benefit from immunotherapy, the TIDE algorithm found that the C3 cluster had a higher TIDE score than the other 2 clusters (Additional file 1: Fig. S1E). The C2 cluster was found to be more sensitive to traditional chemotherapies, such as rapamycin, sunitinib, paclitaxel, sorafenib, crizotinib, and AKT inhibitor VIII (Additional file 1: Fig. S1F).

Determination of crucial NK cell-related genes

We conducted differential gene expression analyses separately on each pair of clusters using the “limma” R package and obtained 1183 common differentially expressed NK-related genes (DE-NKRGs) for the intersection between the results. Furthermore, univariate COX regression analysis of the DE-NKRGs indicated that 518 genes were mainly involved in patient prognosis and included 3 risk-related genes and 515 protective genes (Fig. 2a). Then, the LASSO Cox regression was employed to shrink the scope of the genes and the model was found to be optimal when the value of lambda was 0.0473 (Fig. 2b, c). The expression of 6 genes included 2 risk-related genes (DPYSL3 and SLPI) and 4 protective genes (SLC44A4, ZNF521, LIMCH1, and AHR) was estimated in two cell lines by qRT-PCR (Fig. 2d). The qRT-PCR results exhibited that the risk-related gene DPYSL3 was highly expressed and the protective gene SLC44A4 was lowly expressed in ACHN cells, which was consistent with expectations. Meanwhile, ZNF521, LIMCH1, and AHR expression were upregulated in the ACHN cells compared with the HK2 cells. The SLPI expression was no clear difference between ACHN and HK2 cells (Fig. 2e).

Construction of a NK cell-related risk signature

The selected 6 DE-NKRGs were incorporated into the risk score: $\text{risk score} = -0.375 \times \text{LIMCH1} - 0.384 \times \text{AHR} - 0.287 \times \text{ZNF521} + 0.412 \times \text{DPYSL3} - 0.137 \times \text{SLC44A4} + 0.121 \times \text{SLPI}$. Based on the median value, we separated the patients into low-risk and high-risk groups. It was observed that patients with a high-risk score had a poorer prognosis than those with a

low-risk score (Fig. 3a) [58]. The ROC analysis was conducted to analyze the prognostic efficiency of the risk score. The AUC of the TCGA cohort reached 0.78,95 after 1 year, 0.74,95 after 3 years, and 0.75,95 after 5 years. Similarly, the AUC of the ICGC cohort achieved 0.7,95 after 1 year, 0.69,95 after 3 years, and 0.66,95 after 5 years. Kaplan–Meier analyses of both TCGA and ICGC cohorts consistently showed that low-risk patients tended to have a more favorable outcome (Fig. 3b).

Relationship between the risk score and clinical features, immune microenvironment, and treatment response

We further analyzed the distribution of the clinical features of patients in the TCGA cohort [59]. A remarkable difference exists between the 2 groups in terms of tumor stage. The C2 cluster showed a significantly lower risk score (Additional file 1: Fig. S2A). To elucidate the relationship between the risk score and the immune microenvironment of ccRCC, the MCP-counter tool was used to investigate differences in the infiltration of 10 immune cells between the high- and low-risk groups. The results highlighted that the low-risk group had a higher level of immune cell infiltration (Additional file 1: Fig. S2B) [60]. Moreover, we performed TIDE analysis to further explore the clinical utility of the risk score. The low-risk group possessed a lower TIDE score compared with the high-risk group (Additional file 1: Fig. S2C). In addition, patients in the low-risk group exhibited a higher degree of sensitivity to conventional drugs, such as rapamycin, sunitinib, sorafenib, crizotinib, and AKT inhibitor VIII (Additional file 1: Fig. S2D).

Building a survival decision tree and a predictive nomogram to predict ccRCC survival

Additionally, validated the prognostic model using decision tree analysis integrating risk score and clinicopathological features, including age, gender, T stage, N stage, M stage, stage, and grade. Age, stage, grade, and risk score were entered as inputs into the survival decision tree to obtain 7 risk subgroups (Fig. 4a). Survival analyses also revealed statistically significant differences between the 7 risk subgroups (Fig. 4b). Next, we used univariate and multivariate Cox regression analyses and found that the risk score was the most significant factor for the prediction of ccRCC prognosis (Fig. 4c, d). To create a clinical approach for the prognostic estimation of ccRCC patients, the factors mentioned in the decision tree analysis were further applied to construct a nomogram (Fig. 4e). The results of the nomogram showed that the risk score had a dramatic influence on the survival prediction of ccRCC patients. The calibration plots for 1-year, 3-year, and 5-year

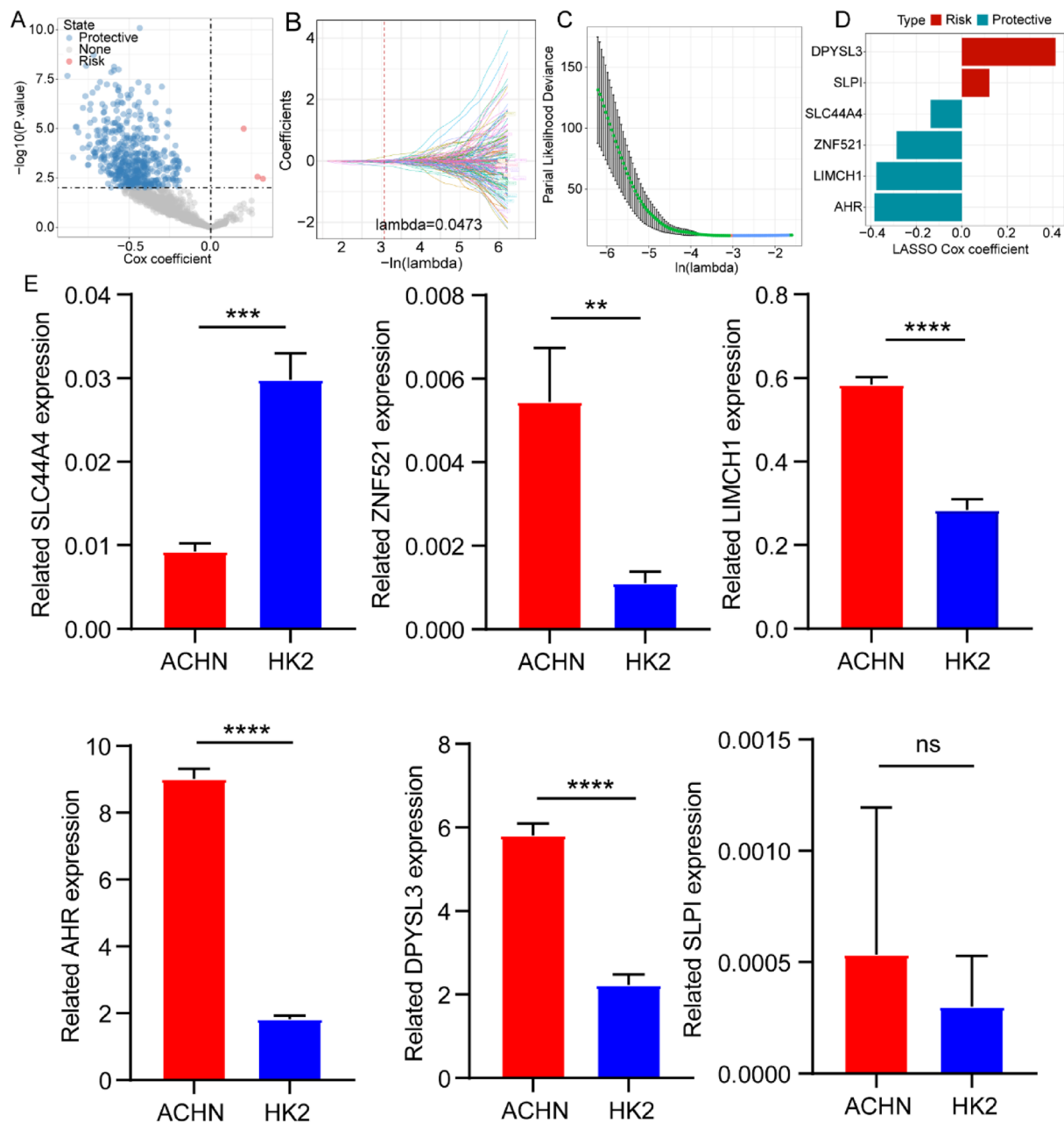


Fig. 2 Construction and validation of a NK cell-related risk score model. **A** Univariate COX regression analysis of the DE-NKRGs in the TCGA database. **B** LASSO coefficient profiles. **C** Lambda selection through tenfold cross-validation. **D** Coefficient of the 6 screened genes. **E** Expression profiles of DPYSL3, SLPI, SLC44A4, ZNF521, LIMCH1, and AHR in the ACHN cells and HK2 cells.

survival probabilities showed high consistency between the results of the constructed nomogram and actual clinical conditions (Fig. 4f). Moreover, the tROC curves with high AUC values above 0.7 indicated that the nomogram and risk score provided an accurate prediction of ccRCC prognosis (Fig. 4g). These results demonstrate the favorable predictive value of our risk score.

Discussion

Emerging evidence suggests that NK cells play essential and dual roles in diverse disease models such as infection, transplantation, autoimmunity, as well as cancer. Studies have reported that NK cells function as crucial components of tumor immunosurveillance, exerting a potent cytolytic effect by recognizing ligands presented on tumor cells and inducing the involvement of a series

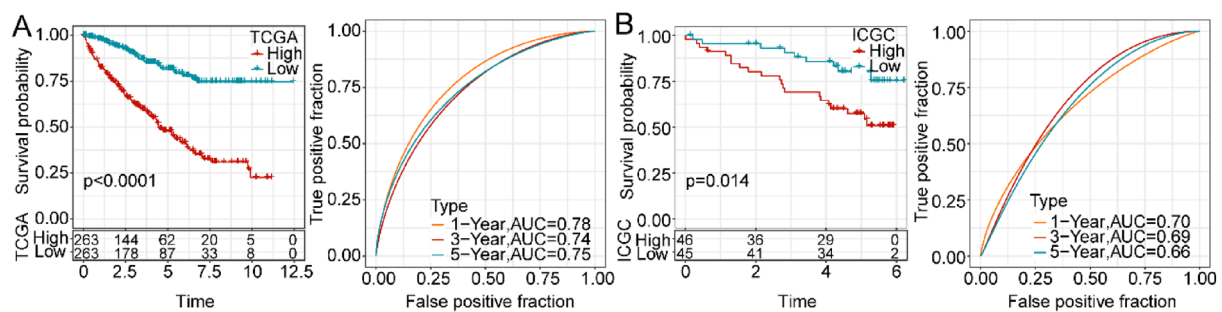


Fig. 3 Exploration of the correlation of risk score with ccRCC prognosis. **A** Kaplan–Meier analysis and ROC curves at 1, 3, and 5 years of high- and low-risk groups in TCGA database. **B** Kaplan–Meier analysis and ROC curves at 1, 3, and 5 years of high- and low-risk groups in ICGC database

of NK activating receptors [61, 62]. For ccRCC, immune-based therapies (including targeted PD-1/PD-L1) have emerged as the main management modality since it has a restricted response to conventional chemotherapy [63–65]. Thus, a more comprehensive understanding of the features of immune cells of ccRCC patients is imperative for developing effective and improved immunotherapies [25].

Research has uncovered the heterogeneity of infiltrating NK cells in ccRCC, revealing their intricate association with tumor metastasis and differences in the efficacy of immunotherapy [66]. Sierra et al. observed an increased expression of PD-L1 on NK cells and a corresponding high infiltration in ccRCC, which paradoxically correlated with worsen survival outcomes of ccRCC patients [67]. Ziblat et al. found that tumor-infiltrating NK cells (TINK) in ccRCC represent an activated residency phenotype, contributing to desensitizing NK cells to tumor cells and further limiting their anti-tumor effect [68].

To identify NK cell-related prognostic biomarkers for ccRCC, we initially identified three prognostic clusters based on NK cell-related gene expression from the TCGA and ICGC databases. Bioinformatics analysis of ccRCC revealed distinct clinicopathological characteristics, prognosis, immune infiltration properties, and therapeutic responses among these three NK cell-related clusters. Risk scores have been proven to allow clinicians to adopt more personalized clinical approaches and facilitate prognostic outcomes as high-throughput genomic technologies become increasingly integrated into clinical practice [69–72]. Zhang et al. structured a risk score model for oral squamous cell carcinoma based on the expression of the Shelterin complex gene (SG) to evaluate the prognosis and immunotherapy responses of patients [73]. Additionally, Cao et al. identified a risk model based on immune-related gene signatures to predict prognosis and guide individualized therapies for advanced

RCC [74]. Considering the distinctive characteristics of the molecular clusters, we constructed a six-gene based NK-related risk score model to explore the association between NK-related genes and ccRCC development. Our research reported that the high-risk score group significantly implicated poorer outcomes, advanced clinical stages, reduced immune cell infiltration, and increased insensitivity to anti-tumor immune responses. Given its role in representing the clinical decision-making processes, we implemented a decision tree model to further validate the performance of risk scores. Importantly, we indicated that a proposed nomogram integrating risk scores with clinical characteristics showed superior effective predictive efficacy for ccRCC prognosis.

Recent advancements in imaging technology and genomics have significantly aided clinical physicians in stratifying risk, selecting treatment plans, developing follow-up strategies, and predicting patient outcomes for various diseases. The combination of radiomics features and genomic data has demonstrated promising applications in clinical settings, such as RCC [75, 76]. In this study, we primarily analyzed NK cell-related gene expression in ccRCC and established a corresponding prognostic model. We validated the model's robustness and efficacy by utilizing public ccRCC patient databases. Based on individual risk characteristics, the model can be utilized to stratify patients, predict treatment responses, and evaluate clinical prognoses. Further integration of our prognostic model with radiomics offers a meaningful direction for future research. By combining clinical radiological information of ccRCC patients, our model holds potential to provide more personalized risk assessment, elevated diagnostic accuracy, and refined treatment plans and follow-up strategies for patients.

However, our research has several limitations. First, the gene expression data used in our study were obtained from online platforms, and there is a lack of data from our own center to validate the constructed prognostic

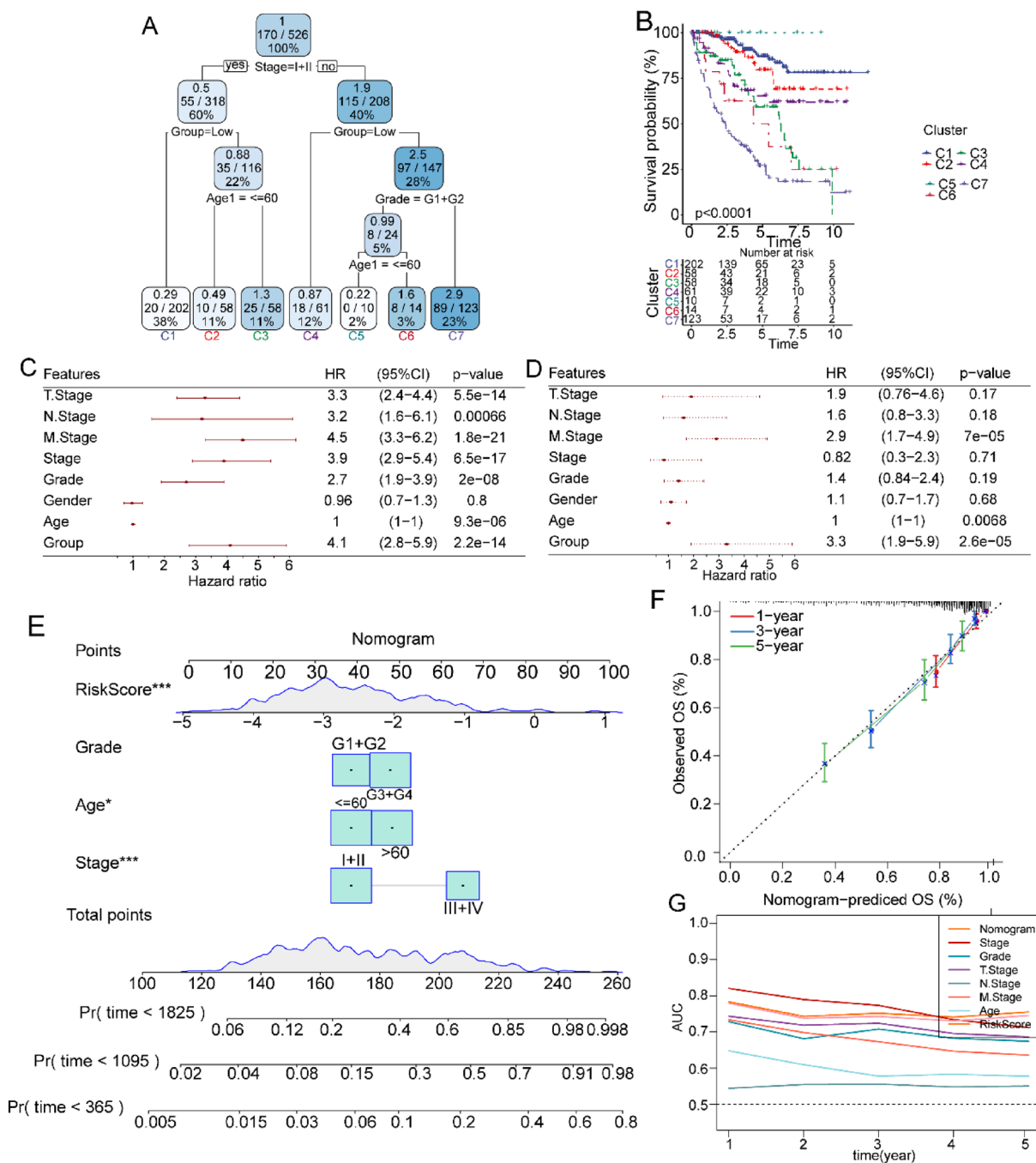


Fig. 4 Establishment of a decision tree and nomogram by combining the risk score and clinical features of TCGA database. **A** Framework of a decision tree. **B** Survival analysis of the 7 clusters obtained using the decision tree. **C** Results of the univariate Cox analysis. **D** Results of the multivariate Cox analysis. **E** The nomogram constructed to predict the survival probabilities. **F** Calibration curves of the nomogram. **G** The ROC curves of the nomogram.

model. Second, we focused only on 6 genes with the most significant correlation with ccRCC prognosis to establish the model. Although we found evidence supporting the importance of the expression and prognosis of these 6 genes, their functional mechanisms during ccRCC

development are worthy of further experimental studies and validation in vivo. The qRT-PCR merely confirmed the mRNA expression profiles of the 6 genes and further analysis is needed to expand the exploration of 6 genes at the protein level and also on the animal models.

Conclusion

Taken together, we identified three distinct molecular clusters and proposed a generalized and robust prognostic model for ccRCC based on NK-related gene signatures. The risk score was confirmed to exert a powerful role for the prediction of ccRCC prognosis and can provide more appropriate guidance for the treatment of ccRCC patients.

Supplementary Information

The online version contains supplementary material available at <https://doi.org/10.1186/s40001-024-01659-0>.

Additional file 1. Fig. S1: Relationship between molecular subtypes and clinical characteristics, immune cell infiltration, immune score, immune checkpoint genes, and treatment sensitivities. **A** Distribution of the clinical characteristics in the 3 molecular clusters. **B** Degree of infiltration of the 10 types of immune cells in the 3 molecular clusters. **C** Immune scores in the 3 molecular clusters. **D** Difference in the expression of immune checkpoint genes in the 3 molecular clusters. **E** Immunotherapy response in the 3 molecular clusters. **F** Sensitivities of traditional chemotherapy in the 3 molecular clusters. **Fig. S2:** Differences in clinical features, immune cell infiltration, immune escape and chemosensitivity between the high- and low-risk groups. Association between the NK cell-related Risk Score and **A** clinical features, **B** immune cell infiltration, **C** immune escape, and **D** chemosensitivity in the TCGA database. **Table S1:** The primer sequences for qRT-PCR.

Acknowledgements

The authors acknowledge the Cancer Genome Atlas (TCGA) and the International Cancer Genome Consortium (ICGC) database for providing access to their invaluable public databases.

Author contributions

QY and DC conducted the study design, methodology, data curation, data analysis, validation, writing, reviewing, and manuscript editing. XZ, YW, and CW performed data analysis, validation, reviewing, and editing of the manuscript. JC conducted the supervision, reviewing, and editing of the manuscript.

Funding

This work was supported by the National Natural Science Foundation of China (82360157), and the Key R&D projects of Zhejiang Department of Science and Technology (2023C04011).

Data availability

The data that support the findings of this study are available from the corresponding author upon reasonable request.

Declarations

Ethics approval and consent to participate

Not applicable.

Consent for publication

Not applicable.

Competing interests

The authors declare that the research was conducted in the absence of any commercial or financial relationships that could be construed as a potential conflict of interest.

Author details

¹Kidney Disease Center, the First Affiliated Hospital, College of Medicine, Zhejiang University, Qingchun Road 79, Hangzhou 310003, China. ²Key Laboratory of Kidney Disease Prevention and Control Technology, Hangzhou, Zhejiang

Province, China. ³Institute of Nephropathy, Zhejiang University, Hangzhou, China. ⁴Zhejiang Clinical Research Center of Kidney and Urinary System Disease, Hangzhou, China.

Received: 11 December 2023 Accepted: 11 January 2024

Published online: 24 January 2024

References

1. Alsaab HO, Sau S, Alzhrani RM, Cheriyan VT, Polin LA, Vaishampayan U, Rishi AK, Iyer AK. Tumor hypoxia directed multimodal nanotherapy for overcoming drug resistance in renal cell carcinoma and reprogramming macrophages. *Biomaterials*. 2018;183:280–94.
2. Hsieh JJ, Purdue MP, Signoretti S, Swanton C, Albiges L, Schmidinger M, Heng DY, Larkin J, Ficarra V. Renal cell carcinoma. *Nat Rev Dis Primers*. 2017;3:17009.
3. Comprehensive molecular characterization of clear cell renal cell carcinoma. *Nature*. 2013;499:43–9.
4. Rini BI, Campbell SC, Escudier B. Renal cell carcinoma. *Lancet*. 2009;373:1119–32.
5. Pan H, Lu W, Zhang M, Liu C. Construction of an interferon regulatory factors-related risk model for predicting prognosis, immune microenvironment and immunotherapy in clear cell renal cell carcinoma. *Front Oncol*. 2023;13:1131191.
6. Hsieh JJ, Le VH, Oyama T, Ricketts CJ, Ho TH, Cheng EH. Chromosome 3p loss-orchestrated VHL, HIF, and epigenetic deregulation in clear cell renal cell carcinoma. *J Clin Oncol*. 2018;36:Jco2018792549.
7. Marona P, Górka J, Mazurek Z, Wilk W, Rys J, Majka M, Jura J, Miekus K. MCP1P1 downregulation in clear cell renal cell carcinoma promotes vascularization and metastatic progression. *Cancer Res*. 2017;77:4905–20.
8. Chevillet JC, Lohse CM, Zincke H, Weaver AL, Blute ML. Comparisons of outcome and prognostic features among histologic subtypes of renal cell carcinoma. *Am J Surg Pathol*. 2003;27:612–24.
9. Ljungberg B, Campbell SC, Choi HY, Jacqmin D, Lee JE, Weikert S, Kiemeny LA. The epidemiology of renal cell carcinoma. *Eur Urol*. 2011;60:615–21.
10. Gudbjartsson T, Hardarson S, Petursdottir V, Thoroddsen A, Magnusson J, Einarsson GV. Histological subtyping and nuclear grading of renal cell carcinoma and their implications for survival: a retrospective nation-wide study of 629 patients. *Eur Urol*. 2005;48:593–600.
11. Cindolo L, Patard JJ, Chiadini P, Schips L, Ficarra V, Tostain J, de La Taille A, Altieri V, Lobel B, Zigeuner RE, et al. Comparison of predictive accuracy of four prognostic models for nonmetastatic renal cell carcinoma after nephrectomy: a multicenter European study. *Cancer*. 2005;104:1362–71.
12. Yang L, Shi L, Fu Q, Xiong H, Zhang M, Yu S. Efficacy and safety of sorafenib in advanced renal cell carcinoma patients: Results from a long-term study. *Oncol Lett*. 2012;3:935–9.
13. Jia Z, Wan F, Zhu Y, Shi G, Zhang H, Dai B, Ye D. Forkhead-box series expression network is associated with outcome of clear-cell renal cell carcinoma. *Oncol Lett*. 2018;15:8669–80.
14. Heng DY, Xie W, Regan MM, Harshman LC, Bjarnason GA, Vaishampayan UN, Mackenzie M, Wood L, Donskov F, Tan MH, et al. External validation and comparison with other models of the international metastatic renal-cell carcinoma database consortium prognostic model: a population-based study. *Lancet Oncol*. 2013;14:141–8.
15. Girgis H, Masui O, White NM, Scorilas A, Rotondo F, Seiwright A, Gabril M, Filter ER, Girgis AH, Bjarnason GA, et al. Lactate dehydrogenase A is a potential prognostic marker in clear cell renal cell carcinoma. *Mol Cancer*. 2014;13:101.
16. Roos FC, Roberts AM, Hwang II, Moriyama EH, Evans AJ, Sybingco S, Watson IR, Carneiro LA, Gedye C, Girardin SE, et al. Oncolytic targeting of renal cell carcinoma via encephalomyocarditis virus. *EMBO Mol Med*. 2010;2:275–88.
17. Heng DY, Xie W, Regan MM, Warren MA, Golshayan AR, Sahi C, Eigl BJ, Ruether JD, Cheng T, North S, et al. Prognostic factors for overall survival in patients with metastatic renal cell carcinoma treated with vascular endothelial growth factor-targeted agents: results from a large, multicenter study. *J Clin Oncol*. 2009;27:5794–9.

18. Qi H, Ohh M. The von Hippel-Lindau tumor suppressor protein sensitizes renal cell carcinoma cells to tumor necrosis factor-induced cytotoxicity by suppressing the nuclear factor- κ B-dependent antiapoptotic pathway. *Cancer Res.* 2003;63:7076–80.
19. Chevrier S, Levine JH, Zanotelli VRT, Silina K, Schulz D, Bacac M, Ries CH, Ailles L, Jewett MAS, Moch H, et al. An immune atlas of clear cell renal cell carcinoma. *Cell.* 2017;169:736–49.e18.
20. Braun DA, Hou Y, Bakouny Z, Ficial M, Sant' Angelo M, Forman J, Ross-Macdonald P, Berger AC, Jegede OA, Elagina L, et al. Interplay of somatic alterations and immune infiltration modulates response to PD-1 blockade in advanced clear cell renal cell carcinoma. *Nat Med.* 2020;26:909–18.
21. Ghatalia P, Gordetsky J, Kuo F, Dulaimi E, Cai KQ, Devarajan K, Bae S, Naik G, Chan TA, Uzzo R, et al. Prognostic impact of immune gene expression signature and tumor infiltrating immune cells in localized clear cell renal cell carcinoma. *J Immunother Cancer.* 2019;7:139.
22. Braun DA, Street K, Burke KP, Cookmeyer DL, Denize T, Pedersen CB, Gohil SH, Schindler N, Pomerance L, Hirsch L, et al. Progressive immune dysfunction with advancing disease stage in renal cell carcinoma. *Cancer Cell.* 2021;39:632–48.e8.
23. Xu WH, Xu Y, Wang J, Wan FN, Wang HK, Cao DL, Shi GH, Qu YY, Zhang HL, Ye DW. Prognostic value and immune infiltration of novel signatures in clear cell renal cell carcinoma microenvironment. *Aging (Albany).* 2019;11:6999–7020.
24. Şenbabaoğlu Y, Gejman RS, Winer AG, Liu M, Van Allen EM, de Velasco G, Miao D, Ostrovskaya I, Drill E, Luna A, et al. Tumor immune microenvironment characterization in clear cell renal cell carcinoma identifies prognostic and immunotherapeutically relevant messenger RNA signatures. *Genome Biol.* 2016;17:231.
25. Kourtis N, Wang Q, Wang B, Oswald E, Adler C, Cherravuru S, Malahias E, Zhang L, Golubov J, Wei Q, et al. A single-cell map of dynamic chromatin landscapes of immune cells in renal cell carcinoma. *Nat Cancer.* 2022;3:885–98.
26. Borcherding N, Vishwakarma A, Voigt AP, Bellizzi A, Kaplan J, Nepple K, Salem AK, Jenkins RW, Zakharia Y, Zhang W. Mapping the immune environment in clear cell renal carcinoma by single-cell genomics. *Commun Biol.* 2021;4:122.
27. Zhang Y, Narayanan SP, Mannan R, Raskind G, Wang X, Vats P, Su F, Hossaini N, Cao X, Kumar-Sinha C, et al. Single-cell analyses of renal cell cancers reveal insights into tumor microenvironment, cell of origin, and therapy response. *Proc Natl Acad Sci USA.* 2021;118:1.
28. Krishna C, DiNatale RG, Kuo F, Srivastava RM, Vuong L, Chowell D, Gupta S, Vanderbilt C, Purohit TA, Liu M, et al. Single-cell sequencing links multiregional immune landscapes and tissue-resident T cells in ccRCC to tumor topology and therapy efficacy. *Cancer Cell.* 2021;39:662–77.e6.
29. Ortaldo JR, Herberman RB. Heterogeneity of natural killer cells. *Annu Rev Immunol.* 1984;2:359–94.
30. Sun K, Alvarez M, Ames E, Barao I, Chen M, Longo DL, Redelman D, Murphy WJ. Mouse NK cell-mediated rejection of bone marrow allografts exhibits patterns consistent with Ly49 subset licensing. *Blood.* 2012;119:1590–8.
31. Gross O, Grupp C, Steinberg C, Zimmermann S, Strasser D, Hainisch-Flögel N, Reindl W, Jonsson H, Huo H, Littman DR, et al. Multiple ITAM-coupled NK-cell receptors engage the Bcl10/Malt1 complex via Carma1 for NF- κ B and MAPK activation to selectively control cytokine production. *Blood.* 2008;112:2421–8.
32. Malarkannan S. The balancing act: inhibitory Ly49 regulate NKG2D-mediated NK cell functions. *Semin Immunol.* 2006;18:186–92.
33. Lai CB, Zhang Y, Rogers SL, Mager DL. Creation of the two isoforms of rodent NKG2D was driven by a B1 retrotransposon insertion. *Nucl Acids Res.* 2009;37:3032–43.
34. Xu D, Han Q, Hou Z, Zhang C, Zhang J. miR-146a negatively regulates NK cell functions via STAT1 signaling. *Cell Mol Immunol.* 2017;14:712–20.
35. Xie G, Dong H, Liang Y, Ham JD, Rizwan R, Chen J. CAR-NK cells: a promising cellular immunotherapy for cancer. *EBioMedicine.* 2020;59:102975.
36. Myers JA, Miller JS. Exploring the NK cell platform for cancer immunotherapy. *Nat Rev Clin Oncol.* 2021;18:85–100.
37. Minetto P, Guolo F, Pesce S, Greppi M, Obino V, Ferretti E, Sivori S, Genova C, Lemoli RM, Marcenaro E. Harnessing NK cells for cancer treatment. *Front Immunol.* 2019;10:2836.
38. Shimasaki N, Jain A, Campana D. NK cells for cancer immunotherapy. *Nat Rev Drug Discov.* 2020;19:200–18.
39. Miyazato K, Hayakawa Y. Pharmacological targeting of natural killer cells for cancer immunotherapy. *Cancer Sci.* 2020;111:1869–75.
40. Nie H, Bu F, Xu J, Li T, Huang J. 29 immune-related genes pairs signature predict the prognosis of cervical cancer patients. *Sci Rep.* 2020;10:14152.
41. Zhang C, Zheng JH, Lin ZH, Lv HY, Ye ZM, Chen YP, Zhang XY. Profiles of immune cell infiltration and immune-related genes in the tumor microenvironment of osteosarcoma. *Aging (Albany).* 2020;12:3486–501.
42. Ascione CM, Napolitano F, Esposito D, Servetto A, Belli S, Santaniello A, Scagliarini S, Crocetto F, Bianco R, Formisano L. Role of FGFR3 in bladder cancer: treatment landscape and future challenges. *Cancer Treat Rev.* 2023;115:102530.
43. Soldierer M, Bister A, Haist C, Thivakaran A, Cengiz SC, Sendker S, Bartels N, Thomitzek A, Smorra D, Hejazi M, et al. Genetic engineering and enrichment of human NK cells for CAR-enhanced immunotherapy of hematological malignancies. *Front Immunol.* 2022;13:847008.
44. Kaifu T, Escalière B, Gastinel LN, Vivier E, Baratin M. B7–H6/NKp30 interaction: a mechanism of alerting NK cells against tumors. *Cell Mol Life Sci.* 2011;68:3531–9.
45. Phung SK, Miller JS, Felices M. Bi-specific and Tri-specific NK cell engagers: the new avenue of targeted NK cell immunotherapy. *Mol Diagn Ther.* 2021;25:577–92.
46. Xie MZ, Tang YP, Hu BL, Li KZ, Li JL, Liang XQ. Percentage of natural killer (NK) cells in peripheral blood is associated with prognosis in patients with gastric cancer: a retrospective study from a single center. *Med Sci Monit.* 2021;27:e927464.
47. Liu Z, Ding M, Qiu P, Pan K, Guo Q. Natural killer cell-related prognostic risk model predicts prognosis and treatment outcomes in triple-negative breast cancer. *Front Immunol.* 2023;14:1200282.
48. Bhattacharya S, Andorf S, Gomes L, Dunn P, Schaefer H, Pontius J, Berger P, Desborough V, Smith T, Campbell J, et al. ImmPort: disseminating data to the public for the future of immunology. *Immunol Res.* 2014;58:234–9.
49. Zhang X, Yang J, Yu X, Cheng S, Gan H, Xia Y. Angiotensin II-induced early and late inflammatory responses through NOXs and MAPK pathways. *Inflammation.* 2017;40:154–65.
50. Quyang W, Jiang Y, Bu S, Tang T, Huang L, Chen M, Tan Y, Ou Q, Mao L, Mai Y, et al. A prognostic risk score based on hypoxia-, immunity-, and epithelial-to-mesenchymal transition-related genes for the prognosis and immunotherapy response of lung adenocarcinoma. *Front Cell Dev Biol.* 2021;9:758777.
51. Becht E, Giraldo NA, Lacroix L, Buttard B, Elarouci N, Petitprez F, Selves J, Laurent-Puig P, Sautès-Fridman C, Fridman WH, et al. Estimating the population abundance of tissue-infiltrating immune and stromal cell populations using gene expression. *Genome Biol.* 2016;17:218.
52. Subramanian A, Tamayo P, Mootha VK, Mukherjee S, Ebert BL, Gillette MA, Paulovich A, Pomeroy SL, Golub TR, Lander ES, et al. Gene set enrichment analysis: a knowledge-based approach for interpreting genome-wide expression profiles. *Proc Natl Acad Sci USA.* 2005;102:15545–50.
53. Yoshihara K, Shahmoradgolji M, Martínez E, Vegesna R, Kim H, Torres-García W, Treviño V, Shen H, Laird PW, Levine DA, et al. Inferring tumour purity and stromal and immune cell admixture from expression data. *Nat Commun.* 2013;4:2612.
54. Fu J, Li K, Zhang W, Wan C, Zhang J, Jiang P, Liu XS. Large-scale public data reuse to model immunotherapy response and resistance. *Genome Med.* 2020;12:21.
55. Liu Y, He M, Wang D, Diao L, Liu J, Tang L, Guo S, He F, Li D. HisgAtlas 1.0: a human immunosuppression gene database. *Database (Oxford).* 2017;2017:1.
56. Zeng J, Li M, Dai K, Zuo B, Guo J, Zang L. A novel glycolysis-related long noncoding RNA signature for predicting overall survival in gastric cancer. *Pathol Oncol Res.* 2022;28:1610643.
57. Maniatis AJ, Folberg R, Hess A, Sefror EA, Gardner LM, Pe'er J, Trent JM, Meltzer PS, Hendrix MJ. Vascular channel formation by human melanoma cells in vivo and in vitro: vasculogenic mimicry. *Am J Pathol.* 1999;155:739–52.
58. Zhang C, Gou X, He W, Yang H, Yin H. A glycolysis-based 4-mRNA signature correlates with the prognosis and cell cycle process in patients with bladder cancer. *Cancer Cell Int.* 2020;20:177.
59. You P, Liu S, Li Q, Xie D, Yao L, Guo C, Guo Z, Wang T, Qiu H, Guo Y, et al. Radiation-sensitive genetic prognostic model identifies individuals at risk for radiation resistance in head and neck squamous cell carcinoma. *J Cancer Res Clin Oncol.* 2023;149:15623–40.

60. Wang M, Zhao X, Zhu D, Liu T, Liang X, Liu F, Zhang Y, Dong X, Sun B. HIF-1 α promoted vasculogenic mimicry formation in hepatocellular carcinoma through LOXL2 up-regulation in hypoxic tumor microenvironment. *J Exp Clin Cancer Res*. 2017;36:60.
61. Waldhauer I, Steinle A. NK cells and cancer immunosurveillance. *Oncogene*. 2008;27:5932–43.
62. Morvan MG, Lanier LL. NK cells and cancer: you can teach innate cells new tricks. *Nat Rev Cancer*. 2016;16:7–19.
63. Rini BI, Plimack ER, Stus V, Gafanov R, Hawkins R, Nosov D, Pouliot F, Alekseev B, Soulières D, Melichar B, et al. Pembrolizumab plus axitinib versus sunitinib for advanced renal-cell carcinoma. *N Engl J Med*. 2019;380:1116–27.
64. Choueiri TK, Motzer RJ. Systemic therapy for metastatic renal-cell carcinoma. *N Engl J Med*. 2017;376:354–66.
65. Posadas EM, Limvorasak S, Figlin RA. Targeted therapies for renal cell carcinoma. *Nat Rev Nephrol*. 2017;13:496–511.
66. Liang Z, Nong F, Zhao J, Wei D, Tang Q, Song J, Meng L. Heterogeneity in NK cell subpopulations may be involved in kidney cancer metastasis. *J Immunol Res*. 2022;2022:6378567.
67. Sierra JM, Secchiari F, Nuñez SY, Iraolagoitia XLR, Ziblat A, Friedrich AD, Regge MV, Santilli MC, Torres NI, Gantov M, et al. Tumor-experienced human NK cells express high levels of PD-L1 and inhibit CD8(+) T cell proliferation. *Front Immunol*. 2021;12:745939.
68. Ziblat A, Iraolagoitia XLR, Nuñez SY, Torres NI, Secchiari F, Sierra JM, Spallanzani RG, Rovegno A, Secin FP, Fuertes MB, et al. Circulating and tumor-infiltrating NK cells from clear cell renal cell carcinoma patients exhibit a predominantly inhibitory phenotype characterized by overexpression of CD85j, CD45, CD48 and PD-1. *Front Immunol*. 2021;12:681615.
69. Zhang R, Liu F. Cancer-associated fibroblast-derived gene signatures predict radiotherapeutic survival in prostate cancer patients. *J Transl Med*. 2022;20:453.
70. Lichtenstein GR, Targan SR, Dubinsky MC, Rotter JI, Barken DM, Princen F, Carroll S, Brown M, Stachelski J, Chuang E, et al. Combination of genetic and quantitative serological immune markers are associated with complicated Crohn's disease behavior. *Inflamm Bowel Dis*. 2011;17:2488–96.
71. Zhang Y, Wang Q, Yang WK, Wang YS, Zhou Q, Lin J, Wei XX, Liang T, Liu T, Fan WT, et al. Development of an immune-related prognostic biomarker for triple-negative breast cancer. *Ann Med*. 2022;54:1212–20.
72. He G, Chen Z, Zhuo S, Tang J, Hao W, Yang K, Yang C. Pyroptosis: a novel signature to predict prognosis and immunotherapy response in gliomas. *Hum Cell*. 2022;35:1976–92.
73. Zhang S, Yu H, Li J, Zhao L, Tan L, Song Q, Sun C. Identification of prognostic and tumor microenvironment by shelterin complex-related signatures in oral squamous cell carcinoma. *Oxid Med Cell Longev*. 2022;2022:6849304.
74. Cao P, Wu JY, Zhang JD, Sun ZJ, Zheng X, Yu BZ, Cao HY, Zhang FL, Gao ZH, Wang W. A promising prognostic risk model for advanced renal cell carcinoma (RCC) with immune-related genes. *BMC Cancer*. 2022;22:691.
75. Ferro M, Musi G, Marchioni M, Maggi M, Veccia A, Del Giudice F, Barone B, Crocetto F, Lasorsa F, Antonelli A, et al. Radiogenomics in renal cancer management-current evidence and future prospects. *Int J Mol Sci*. 2023;24:1.
76. Ferro M, Crocetto F, Barone B, Del Giudice F, Maggi M, Lucarelli G, Busetto GM, Autorino R, Marchioni M, Cantiello F, et al. Artificial intelligence and radiomics in evaluation of kidney lesions: a comprehensive literature review. *Ther Adv Urol*. 2023;15:17562872231164804.

Publisher's Note

Springer Nature remains neutral with regard to jurisdictional claims in published maps and institutional affiliations.